Optimal Cutting Parameters to Reduce Power Consumption in Face Milling of a Cast Iron Alloy for Environmental Sustainability

Xiaona Luan, Song Zhang and Gaoli Cai

Abstract In the perspective of energy saving, the power consumption in the process of CNC (Computer numerical control) machining is closely related to the environmental issues. Therefore, it is especially important to optimize the cutting parameters to reduce the power consumption. In this paper, the power consumption which is determined by the cutting parameters in the face milling process of a cast iron alloy is researched. First, characteristics of machine tool power consumption were studied and the relationship between power consumption and cutting forces was described qualitatively. Secondly, a power consumption monitoring system was built to monitor and record the power consumption in real time during a face milling process. Secondly, according to central composite design (CCD), a total of 27 experiments were carried out to reveal the relationship between the power consumption and process parameters. Finally, the milling parameters were optimized by means of response surface methodology (RSM). The results indicate that the power consumption of P_M and P_Y can be saved by 38.55 and 28.23 % under the cutting condition of optimized parameters, and the surface quality is insured simultaneously.

Keywords Power consumption · Optimization · Cutting parameters · A cast iron alloy · Face milling

X. Luan · S. Zhang (✉) · G. Cai
Key Laboratory of High Efficiency and Clean Mechanical Manufacture (Ministry of Education); School of Mechanical Engineering, Shandong University, Jinan 250061, China
e-mail: zhangsong@sdu.edu.cn

X. Luan
e-mail: xiaona0412@126.com

G. Cai
e-mail: 313368180@qq.com

R. Setchi et al. (eds.), *Sustainable Design and Manufacturing 2016*,
Smart Innovation, Systems and Technologies 52,
DOI 10.1007/978-3-319-32098-4_12

1 Introduction

The improvement of environment and energy efficiency is associated with development of industry technology. Power efficiency, as a global concept in the engineering field, has been focused on by both the company and government while it can influence the environment directly or indirectly [1]. Previous research showed that two-thirds of the power energy is used in industry field in China. Therefore, the research about power efficiency is becoming considerably important [2].

During metal removal process, relative motions between the cutting tool and the workpiece are realized by main motor and servo motors, which can provide power and torque by consuming electricity. If a component of machine system lacks dynamic stiffness or damping, displacements and forces become higher at each tooth pass and the process becomes unstable [3]. So servo motors are used in a control loop system for these error compensations and consume little electricity during the machining process.

The previous researches pointed out that power consumption is associated with many conditions [4, 5]. Some research has been conducted to evaluate the environmental impacts of machining [6, 7]. In general, the methodologies of energy-efficient modeling of machining systems can be divided into three different levels: machine tool level, component level, and system level [8]. Bi and Wang pointed out that machining energy usage is solely based on specific cutting energy [9]. In order to understand and evaluate the specific cutting energy, the therblig-based energy supply modeling was proposed [10]. Mesquita et al. [11] established an approach to optimize the cutting parameters in turning in order to minimize the production cost and machining time. Response surface methodology (RSM) was widely used in the fields of optimization of cutting parameters [12], power consumption and tool life [13].

Metal removal process is realized by spindle motion and feed motions, and power consumptions of these motions vary from different combination of cutting parameters. Dividing total power into each axial motor's power is benefit for analyzing power consumption of specific motor during machining process and could accurately find large-power machining steps, and then optimized them. By now, few researches investigated real time power consumption of spindle motion and feed motions' driven axis.

The objective of the present research is to find the influence of cutting parameters on power consumption, and then optimized to decreasing the power consumption by RSM. First, the relationship between power consumption and cutting forces was described qualitatively. Secondly, according to central composite design (CCD), a total of 27 experiments were carried out to reveal the relationship between the power consumption and cutting parameters. Finally, the milling parameters were optimized by RSM to minimize the power consumption.

2 Relationship Between Power Consumption and Cutting Force

2.1 Characteristics of Machine Tool Power Consumption

The power consumption of machine tool is usually divided into two components, the cutting power consumption which is caused by removing material and the auxiliary power consumption which is caused by auxiliary equipment during idle process. Cutting power consumption is variable which is related to the material properties, cutting parameters, cutting conditions and tool conditions. There is a complex dynamic interaction and coupling effect between these relevant variables. Power consumption curve is usually made up with dynamic balance equation and stationary state equation alternately, which can be expressed as follows:

$$f_{pi}(t) = \begin{cases} P_i^{\mathrm{D}}(t) & i \in \{\mathrm{D}\} \\ P_i^{\mathrm{U}}(t) & i \in \{\mathrm{U}\} \\ P_i^{\mathrm{C}}(t) & i \in \{\mathrm{C}\} \end{cases} \tag{1}$$

where $P_i^{\mathrm{D}}(t)$ is the input power consumption function of the machine tool starting/braking, $P_i^{\mathrm{U}}(t)$ is the idling power consumption function during the engage and retract process, $P_i^{\mathrm{C}}(t)$ is the input power consumption function of the machining process.

2.2 Power Modeling Method of the Three Types Consumption

The power consumption of machine tool starting/braking $P_i^{\mathrm{D}}(t)$, idling process $P_i^{\mathrm{U}}(t)$, and material removing process $P_i^{\mathrm{C}}(t)$ has their own characteristics and different influencing factors. $P_i^{\mathrm{D}}(t)$ and $P_i^{\mathrm{U}}(t)$ are influenced by the characteristics of machine tool, while $P_i^{\mathrm{C}}(t)$ has some correlation with cutting parameters cutting condition. So the mathematical models of them are studied respectively as follows.

(1) Input power consumption function of the machine tool starting/braking $P_i^{\mathrm{D}}(t)$.

The process of machine tool starting/braking is usually unstable, which makes building of the dynamic balance equation more complex and difficult. But during starting, there's no cutting power, and $P_i^{\mathrm{D}}(t)$ is decided by the structure of machine tool itself and has no effect of the workpiece. When a machine tool is working in a certain speed, the idling power is always constant. In another word, idling power

consumption curve during the engage and retract process is almost a straight line. Besides, the value of idling power has no relation with the workpiece. Then the method of building $P_i^{\mathrm{U}}(t)$ is similar with the $P_i^{\mathrm{D}}(t)$, and the sample database of $P_i^{\mathrm{U}}(\mathrm{t})$ is built up based on some experimental data in different spindle speed n.

(2) Idling power consumption function during the engage and retract process $P_i^{\mathrm{U}}(t)$.

A machine tool idling feature could be expressed by the following equation, which is a stationary state function correlated with the spindle speed n, then $P^{\mathrm{U}}(t) = P^{\mathrm{U}}(n)$.

When a machine tool is working in a certain speed, the idling power is always constant. In another word, idling power consumption curve during the engage and retract process is almost a straight line. Besides, the value of idling power has no relation with the workpiece. Then the method of building $P_i^{\mathrm{U}}(t)$ is similar with the $P_i^{\mathrm{D}}(t)$, and the sample database of $P_i^{\mathrm{U}}(t)$ is built up based on some experimental data in different spindle speed.

(3) Input power consumption function of the machining process $P_i^{\mathrm{C}}(t)$.

Power consumption during face milling process is usually calculated by the following function $P_i^{\mathrm{C}}(t) = P_{ui}(t) + \alpha P_{ci}(t)$. Where $P_{ui}(t)$ is power of auxiliary equipment, and value of $P_{ui}(t)$ is just a constant. $P_{ci}(t)$ is cutting power function. The feature of $P_i^{\mathrm{C}}(t)$ is similar with $P_{ci}(t)$, So study of $P_{ci}(t)$ is very important.

The cutting power consumption $P_{ci}(t)$ can be divided into three parts, i.e., cutting power of spindle P_{m}, power of feed motion P_{f}, and power consumed by auxiliary systems P_{ux} and P_{uz}. P_{m} and P_{f} are affected by the cutting parameters and workpiece material. So they could be decreased by optimizing the cutting parameters. As shown in Fig. 2, during the face milling process, the cutting force change with the chip thickness decreasing from the maximum to zero over a spindle revolution. In the process of material removal, the tool tooth has to withstand instantaneous tangential component F_{t}, instantaneous radial component F_{r}, and instantaneous axial component F_{a} (cutter system) [14]. Once three force components F_{x}, F_{y}, and F_{z} acting on the face milling cutter (table system) in the Cartesian coordinate system are determined by experimental results, three cutting forces F_{t}, F_{r}, and F_{a} (cutter system) on the tooth-workpiece contact point can be expressed through a coordinate transformation.

$$\begin{bmatrix} F_{\mathrm{t}} \\ F_{\mathrm{r}} \\ F_{\mathrm{a}} \end{bmatrix} = \begin{bmatrix} -\sin\varphi(t) & \cos\varphi(t) & 0 \\ \cos\varphi(t) & \sin\varphi(t) & 0 \\ 0 & 0 & 1 \end{bmatrix} \begin{bmatrix} F_{\mathrm{x}} \\ F_{\mathrm{y}} \\ F_{\mathrm{z}} \end{bmatrix} \quad \varphi_{\mathrm{st}} < \varphi(t) < 180^{\circ} \tag{2}$$

During face milling process (Fig. 1), the milling cutter made a feed motion along Y direction, the motion velocity along X and Z direction was zero. The feed rate was very slightly, and the power consumption of feed motion P_{f} was small which caused by F_{y}.

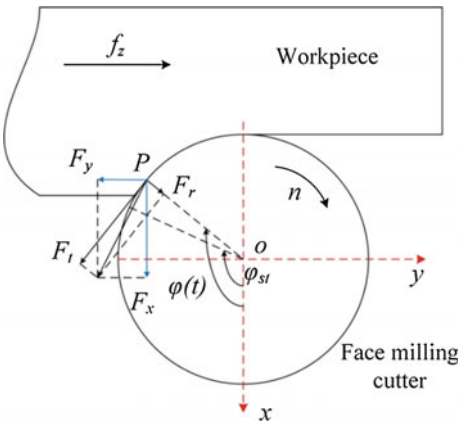

Fig. 1 Schematic view of face milling process

$$P_f = F_y \cdot v_f = F_y \cdot nf_z \tag{3}$$

where F_y is cutting force component along direction of feed (cutting system), v_f is feeding speed (m/min).

The cutting power of spindle P_m is related with the main cutting force F_t.

$$P_m = \frac{F_t \cdot v_c}{1000 \times 60} = \frac{F_t \cdot 2\pi nR}{1000 \times 60} \text{ (W)} \tag{4}$$

where F_t is instantaneous tangential component (N), v_c is cutting speed (m/min), n is the spindle speed (r/min), R is the radius of face milling cutter (mm).

3 Experimental Details

3.1 Workpiece Material, Cutting Tool and Machine Tool

The material of workpiece is a cast iron alloy, which added a small quantity of alloy element Cu, Cr and Sn into the conventional cast alloy HT-250. Rectangular blocks of the workpiece were prepared in the dimensions of 100 × 50 × 25 mm and the surface materials of workpiece were removed. Cutting tools used in the experiments were Seco face milling cutters (F40M) and tool holder was Seco R220.43-0063-07W whose diameter reached 63 mm.

The face milling experiments were performed on a three-axis vertical machining center (Daewoo, ACE-V500) under dry conditions, which has a total power of 30 kW. The main spindle, X, Y, and Z axis are driven by four motors whose rated

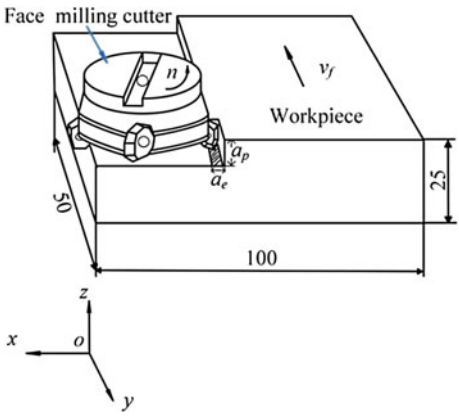

Fig. 2 Schematic of milling process

Table 1 Design of experiments by CCD

Level	1	2	3	4	5
v_c (m/min)	77.5	105.0	132.5	160.0	187.5
f_z (mm/z)	0.13	0.25	0.38	0.50	0.63
a_p (mm)	0.2	0.9	1.6	2.3	3.0
a_e (mm)	0.05	0.95	1.85	2.75	3.65

power are 15, 3.8, 3.8 and 3.8 kW respectively. During the face milling experiments, the power consumption of each electric motor was measured separately. Down milling along the Y axis was used to remove the materials (Fig. 2).

3.2 Design of Face Milling Experiments

In the present experiment, RSM was used for analyzing the effect of simultaneous variations of four cutting parameters (v_c, f_z, a_p and a_e) on energy consumption. Based on CCD, a total of 27 experiments (designed by Table 1) with 5 levels for each of the 4 factors were carried out. The optimization was done by the Design-Expert software, which combines experimental design, data analysis, visual model output and optimization of results. Finally, a feasible combination of v_c, f_z, a_p and a_e can be acquired, which satisfies the minimum energy criterion. The formula used for the regression of the experimental data is quadratic and can be expressed by Eq. (5).

$$Y = \sum_{i=1}^{n}\sum_{j=1}^{n} a_{ij}x_i x_j + \sum_{i=1}^{n} b_i x_i + c \tag{5}$$

3.3 Power Analyzing System

Power consumptions of four specific motors were measured by a power analyzing system (showed in Figs. 3 and 4), which was built up with a NI-9220 data acquisition card installed in a NI-cDAQ 9174 4-slot USB chassis. Each of the four electric motor's working power was measured by a voltage sensor (LV25-P) and a current sensor (LA55-P). Figure 4 showed the principle of the power analyzing system, while Fig. 3 visually showed how every part of experimental equipment was connected.

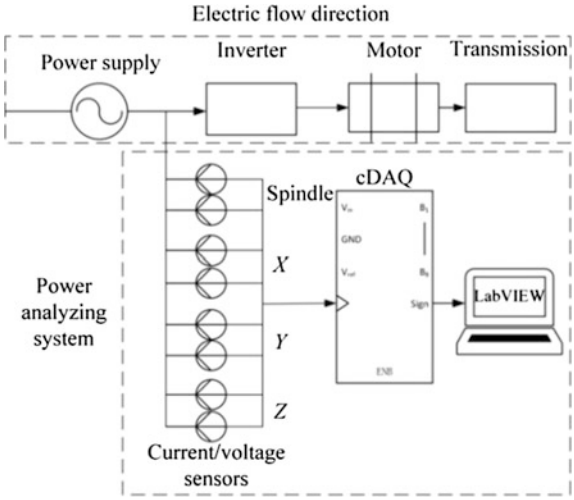

Fig. 3 Schematic of the monitoring system

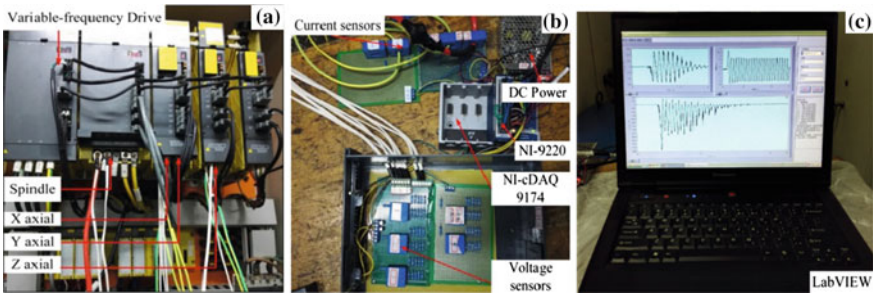

Fig. 4 Physical diagram of power analyzing system

4 Results and Discussions

4.1 Results and Second Order RSM Model Prediction Model Optimization

In the experiment, line voltage U_L and line current I_L were measured to get the motor power of each phase P_L. Then the power P of each motor can be calculated from Eq. (6),

$$P = \sqrt{3} U_L I_L \cos \varphi \tag{6}$$

where φ is the power factor with the value of 0.8. Form the results, it is obvious that P_M and P_Y are much higher than that of P_X and P_Z. But the Z axial motor's power was up to 2200 W at the time of starting, that's because the cutter was far away from the workpiece and closing speed reached 3000 m/min. Therefore, P_M and P_Y are the objectives to be optimized combined with surface roughness Ra, which was measured by an optical profiler Veeco-NT9300.

In the process of optimization, the responses do not have equal importance. The most important response are P_M and P_Y, followed by the surface roughness Ra. The free variables of each experimental factor and power consumption were transformed to the matrix form. The relationship between the power consumption and cutting parameters was established through the least square method. The final mathematical models of P_M and P_Y are given below:

$$\begin{aligned} P_M = &-22.07 v_c - 3515.94 f_z - 1378.73 a_p + 1513.92 a_e + 22.8 v_c f_z - 8.357 v_c a_e \\ &+ 1610.9 f_z a_p - 585.1 f_z a_e + 157.4 a_p a_e + 0.11 v_c^2 + 260.9 a_p^2 \end{aligned} \tag{7}$$

$$\begin{aligned} P_Y = &\ 13.15 v_c - 370.05 f_z + 53.32 a_p + 485.34 a_e - 1.84 v_c a_e \\ &- 324.14 f_z a_e + 97.49 f_z^2 \end{aligned} \tag{8}$$

The experiments for significance of the regression and individual model coefficients were performed to verify the goodness of fit for the obtained model. The normal probability plots of the residuals vs. the predicted response for the power consumption are plotted in Figs. 5 and 6. The data closely follows the straight line. The null hypothesis is that the data distribution law is normal and the alternative hypothesis is that it is abnormal. When the P-value is greater than 0.05 (level of significance), the null hypothesis can't be rejected.

The results of analysis of variance (ANOVA) are listed in Tables 2 and 3. In which, the sum of squares is used to estimate the square of deviation from the grand mean. F-value is an index used to check the adequacy of the model in which calculated value of F should be greater than the F-table value. Table 2 shows that $R^2 = 0.853$, which indicated that satisfaction of Eq. (7) was 85.3 % and $R^2 = 0.853$

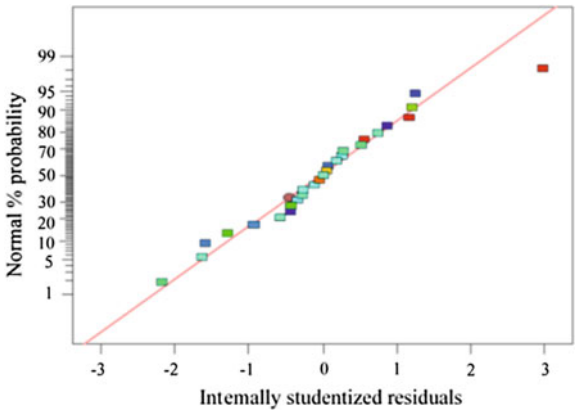

Fig. 5 Residual analysis result (Eq. 7)

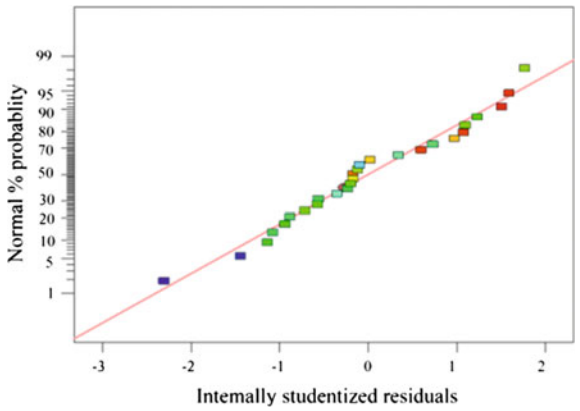

Fig. 6 Residual analysis result (Eq. 8)

Table 2 ANOVA for response surface quadratic model of Eq. (7)

Source	Sum_s	df	Mean_s	F	Prob > F	Significance	R^2
Model	6.54E+006	14	4.67E+005	4.98	0.0042	****	0.853
v_c	2863.399	1	2863.399	0.03	0.8643	–	
f_z	15509.45	1	15509.45	0.17	0.6917	–	
a_p	1659501	1	1659501	17.66	0.0012	*****	
a_e	2962703	1	2962703	31.54	0.0001	*****	
$v_c \times a_e$	684479.1	1	684479.1	7.29	0.0193	***	
$f_z \times a_p$	317886.8	1	317886.8	3.38	0.0907	**	
a_p^2	348670.8	1	348670.8	3.71	0.0781	**	

Table 3 ANOVA for response surface quadratic model of Eq. (8)

Source	Sum_s	df	Mean_s	F	Prob > F	Significance	R^2
Model	1.14E+005	10	11430.51	1.09	0.0056	*****	0.911
v_c	38491.25	1	38491.25	3.66	0.0238	***	
f_z	4377.78	1	4377.78	0.42	0.5280	–	
a_p	220.10	1	220.10	0.02	0.0068	****	
a_e	1739.10	1	1739.10	0.17	0.6897	–	
$v_c \times a_e$	33042.15	1	33042.15	3.14	0.0954	**	
f_z^2	38491.25	1	38491.25	3.66	0.0138	***	

in Table 3. The factors of a_p, a_e, and $v_c \times a_e$ were much more significant than others. The interaction of $f_z \times a_p$ had some effect on spindle power consumption. Table 2 shows "Lack of Fit F-value" of 23.69 implies Lack of Fit is significant. There is only a 4.12 % chance that a "Lack of Fit F-value" this large could occur due to noise. Table 3 shows "Lack of Fit F-value" of 0.81 implies "Lack of Fit" is not significant relative to the pure error. There is a 67.94 % chance that a "Lack of Fit F-value" this large could occur due to noise. From the above analysis, it has been asserted that the developed Eqs. (7) and (8) are well within the limits and can be used for the prediction of responses P_M and P_Y.

4.2 Parameters Optimization Based on RSM

Cutting parameters of v_c, f_z, a_p and a_e are the major milling parameters that are considered in these experiments for optimizing the power consumption. In this work, the multiple performance optimization of milling parameters is carried out using RSM based on desirability function approach. The optimal goal sets and limits and the importance of the factors are presented in Table 4.

In desirability-based approach, different best solutions are obtained and the solution with high desirability is preferred. The solutions are sorted with the most

Table 4 Goals set and limits used for optimization

Factors and responses	Goal	Min.	Max.	Lower	Upper	Importance
v_c	Is in range	105	160	1	1	3
f_z	Is in range	0.25	0.5	1	1	3
a_p	Is in range	0.9	2.3	1	1	3
a_e	Is in range	0.95	2.75	1	1	3
P_M	Minimize	3452	5295	1	2	3
P_Y	Minimize	591	980	1	2	3
Ra	Minimize	500	2000	1	1	3

Table 5 Global solutions for optimization

No.	v_c (m/min)	f_z (mm/z)	a_p (mm)	a_e (mm)	P_M (W)	P_Y (W)	Ra (nm)	Desirability
1	105.02	0.42	0.90	0.95	3452.96	702.585	303.94	0.897
2	105.00	0.42	0.91	0.95	3452.96	702.744	306.00	0.897
3	105.13	0.42	0.90	0.95	3446.55	703.038	309.38	0.896
4	105.00	0.42	0.90	0.96	3452.95	702.952	311.83	0.896

desirable first (Table 5). For example, the input factors are set at range, thus preventing extrapolation. From the analysis of the results, a group of optimal parameters obtained for machining is: v_c of 105.02 m/min, f_z of 0.42 mm/tooth, a_p of 0.90 mm, and a_e of 0.95 mm which could result in a minimum spindle power of 3452.96 W and Y axial power of 702.585 W, while surface roughness is insured with the value of 303.94 nm.

The 3D surface response figure visually showed the effects of the cutting parameters on responses. Interactions of a_p and a_e on spindle power is presented in Fig. 7, which shows that the increase of a_e and a_p increases the desirability and vice versa. In this condition, f_z and v_c are constant: f_z = 0.38 mm/tooth, v_c = 132.50 m/min. The graph is corresponding with the ANOVA results in Table 2. Thus, the power consumption is better at lower cutting speed and axial depth of cut. Interactions of v_c and a_p on Y axial power is presented in Fig. 8, which clearly displays that the Y axial power increases with increase in the effect of a_p and v_c. Results indicated that P_Y becomes lower while the a_p and v_c are all at a higher value. The graph is corresponding with the ANOVA results in Table 3. Thus, the power consumption is better at lower cutting speed and depth of cutting.

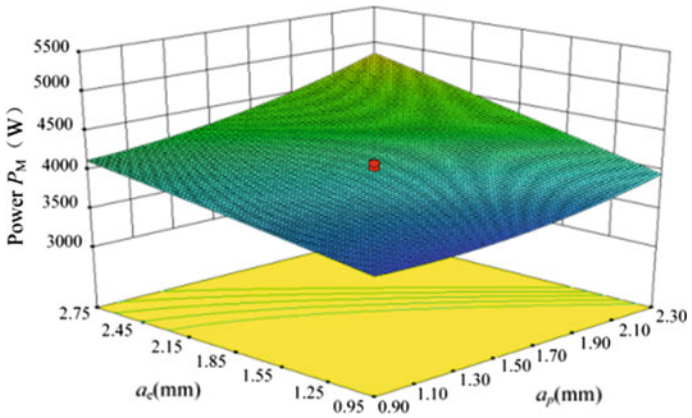

Fig. 7 3D plot of interaction of $a_p \times a_e$ on P_M

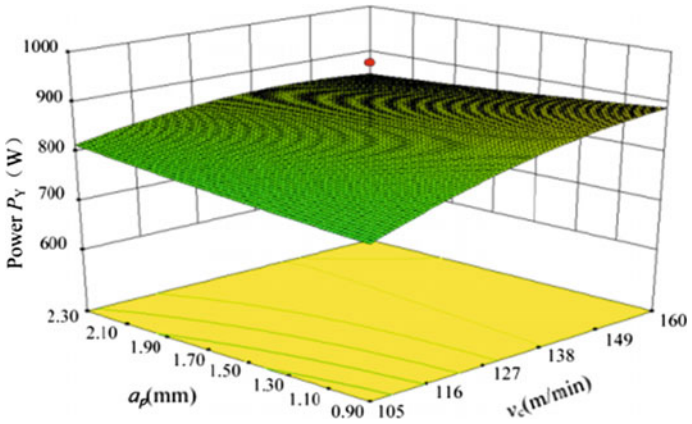

Fig. 8 3D plot of interaction of $v_c \times a_p$ on P_Y

Interaction of $f_z \times a_e$ on Ra is presented in Fig. 9, similarly influence of $a_p \times a_e$ on Ra in Fig. 10, which clearly displays that f_z, a_p, and a_e have an even greater impact on Ra. Dividing the total power consumption into four axial powers makes it easier to determine the optimal objection and simplifies the analysis process.

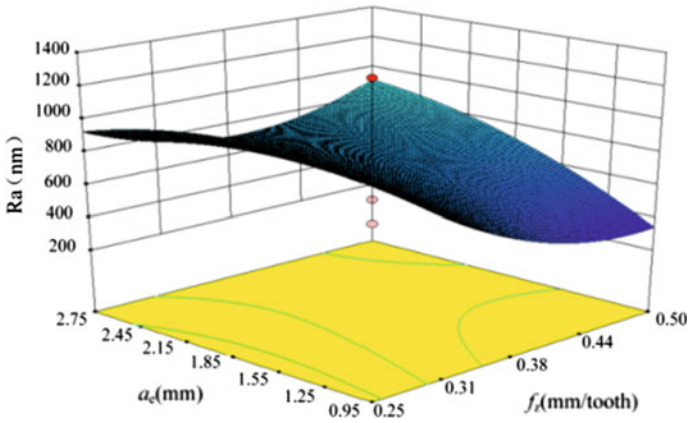

Fig. 9 3D plot of interaction of $f_z \times a_e$ on Ra

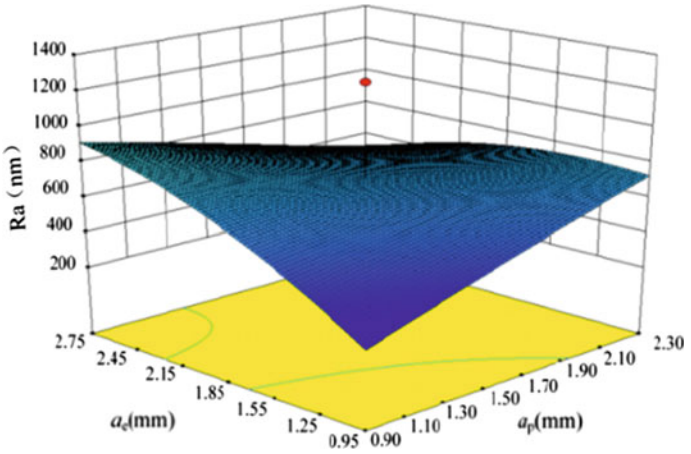

Fig. 10 3D plot of interaction of $a_p \times a_e$ on Ra

5 Conclusions

In this paper, the application of RSM for modeling the influence of cutting parameters on the power consumption of a face milling process is presented. Quadratic mathematical models based on RSM are developed using the results of experiment. Parameters of v_c, f_z, a_e and a_p as the major influence of the power consumption are considered to optimize the power efficiency during machining process. The following conclusions are drawn from the present investigation.

(1) The liner factors a_p, a_e, quadratic factor a_p^2 and the interactive factor $v_c \times a_e$ factors that can affect the spindle power. The significant factor on spindle power P_M is a_e.
(2) The liner factors v_c, a_p, quadratic factor ${f_z}^2$ and the interactive factor $v_c \times a_e$ factors that can affect the Y axial power. The significant factor on Y axial power P_Y is a_p.
(3) The optimal combination of cutting parameters are 105.02 m/min, 0.42 mm/tooth, 0.90 mm, 0.95 mm for v_c, f_z, a_p and a_e, which realized low power consumption and the surface roughness is insured.

Acknowledgements This work is supported by National Major Science and Technology Project: High-end CNC Machine Tools and Basic Manufacturing Equipments (Grant No. 2015ZX04003-005).

References

1. Park, Y.J., Lee, G.B.: Analysis of energy efficiency and productivity in dry process in PCB manufacturing. Int. J. Preci. Engin. Manuf. **14**(7), 1213–1221 (2013)
2. IEA 2015: World Energy Outlook 2015. http://www.worldenergyoutlook.org/
3. de Lacalle, N.L.: Aitzol Lamikiz Mentxaka, Machine Tools for High Performance Machining, pp. 85–108. Springer Science & Business Media, Berlin (2008)
4. Hanafi, I., Khamlichi, A., Cabrera, F.M., Almansa, E., Jabbouri., A.: Optimization of cutting conditions for sustainable machining of PEEK-CF30 using TiN tools. J. Clean. Prod. **33**, 1–9 (2013)
5. Diaz, N., Choi, S., Helu, M., Chen, Y., Jayanathan, S., Yasui, Y.: Machine tool design and operation strategies for green manufacturing. Procedia CIRP **14**, 612–620 (2010)
6. Dahmus, J.B., Gutowski, T.G.: An environmental analysis of machining. In: Proceedings of IMECE2004 ASME International Mechanical Engineering Congress and RD&D Expo-Anaheim, pp. 13–19 (2004)
7. Zolgharni, M., Jones, B.J., Bulpett, R., Anson, A.W., Franks, J.: Energy efficiency improvements in dry drilling with optimized diamond-like carbon coatings. Diam. Relat. Mater. **17**(7), 1733–1737 (2008)
8. Yingjie, Z.: Energy efficiency techniques in machining process: a review. Int. J. Adv. Manuf. Technol. **71**(5–8), 1123–1132 (2014)
9. Bi, Z.M., Wang, L.: Optimization of machining processes from the perspective of energy consumption: A case study. J. Manufact. Syst. **31**(4), 420–428 (2012)
10. Lv, J., Tang, R., Jia, S.: Therblig-based energy supply modeling of computer numerical control machine tools. J. Clean. Prod. **65**, 168–177 (2014)
11. Mesquita, R., Krasteva, E., Doytchinov, S.: Computer-aided selection of optimum machining parameters in multipass turning. Int. J. Adv. Manuf. Technol. **10**(1), 19–26 (1995)
12. Fuad, M.M.M.: Multi-objective Optimization for Clustering Microarray Gene Expression Data-A Comparative Study, Agent and Multi-Agent Systems: Technologies and Applications. Springer International Publishing, Berlin, pp. 123–133 (2015)
13. Bhushan, R.K.: Optimization of cutting parameters for minimizing power consumption and maximizing tool life during machining of Al alloy SiC particle composites. J. Clean. Prod. **39**, 242–254 (2013)
14. Zhang, S., Li, J.F., Sun, J.: Tool wear and cutting forces variation in high-speed end-milling Ti-6Al-4 V alloy. Int. J. Adv. Manuf. Technol. **46**(1–4), 69–78 (2010)